Possible superconductivity in hole-doped BC_3

Filipe J. Ribeiro and Marvin L. Cohen
Department of Physics, University of California, Berkeley, California 94720, USA
and Material Sciences Division, Lawrence Berkeley National Laboratory, Berkeley, California 94720, USA
(Received 28 January 2004; published 23 June 2004)

In this work the superconducting transition temperature of hole-doped BC_3 was studied. The total energy, phonon frequencies, and electron-phonon couplings were calculated for different hole doping levels using the *ab initio* pseudopotential method within the local density approximation. The harmonic and anharmonic phonon frequencies were calculated by using the frozen-phonon approximation. As in MgB_2, the electron-phonon coupling between the electronic states in the σ bands and phonon modes associated with bond stretching was found to be very strong. The calculation predicts that the superconducting temperature will increase as a function of doping level.

DOI: 10.1103/PhysRevB.69.212507 PACS number(s): 74.10.+v, 71.15.Mb, 74.25.Kc, 63.20.Ry

In the past few years a great deal of research has been devoted to the study of superconductivity in MgB_2.[1–6] The relatively high superconducting temperature of 39 K for this material is found to be related to the strong electron-phonon (EP) coupling of the E_{2g} B-B bond stretching phonon modes with the in-plane σ-bonding electronic states.[2–4,6]

The purpose of this work is to demonstrate the possibility of superconductivity in BC_3 (Refs. 7–10) which is a graphitelike metallic material related to MgB_2. The compound BC_3 is synthesized using the chemical reaction of boron trichloride and benzene.[7] As is the case for graphite, BC_3 is a layered material where each layer has hexagonal symmetry with eight atoms per unit cell (see Fig. 1). Recent first principle calculations[11] have shown that the stacking of the BC_3 layers is not as similar to graphite as one may expect. There are at least two stable equilibrium stackings *AB* and *ABC* with 16 and 8 atoms per unit cell, respectively. The *AB* stacking is the energy minimum of all the studied stackings and electronically it is a semiconductor, while the *ABC*-stacking ranks second in energy with an energy difference of 1.4 meV/atom, and it is a metal. Because of this small energy difference and the fact that experimentally BC_3 is a metal, it is expected that the structure, as synthesized experimentally, is a combination of both stackings. In this work the metallic *ABC*-stacking configuration with eight atoms per unit cell is used.

The total energy, phonon frequencies, and EP coupling calculations reported here are based on *ab initio* pseudopotentials[12] within the local density approximation (LDA). The Ceperley-Alder functional[13] for the exchange and correlation energy was used. The wave functions of the valence electrons were expanded in a plane wave basis with an energy cutoff of 70 Ry, and the interaction with the ionic cores was modeled by separable,[14] norm conserving Troullier-Martins[15] pseudopotentials. The total energy is calculated by a numerical integration over the Brillouin zone sampled over a $9\times9\times6$ *k*-point grid, and the forces are given by the Hellmann-Feynman theorem.

The phonon frequencies were calculated using the frozen-phonon approach.[16,17] The dynamical matrix was calculated and diagonalized to obtain the 21 optical phonon eigenmodes at the Γ point. A calculation of the phonon dispersion and EP coupling for the entire Brillouin zone (BZ) is beyond the scope of this work. Since the BZ in BC_3 is roughly 2×2 smaller than in MgB_2, we are assuming that the EP coupling at Γ is representative of the full BZ. If the EP coupling is peaked at Γ, then the superconducting transition temperature T_c can be overestimated.

Anharmonic effects, which play a strong role in the superconductivity of MgB_2,[6] are taken into account. The variation of the total energy as a function of a frozen-phonon amplitude was fit to a fourth-order polynomial. The harmonic phonon frequency is obtained from the quadratic coefficient of the fit, while the anharmonic frequency is given by the energy difference between the two lowest quantum-mechanical vibrational states.

The hole-doped calculations have been performed by reducing the total number of electrons in the system when the

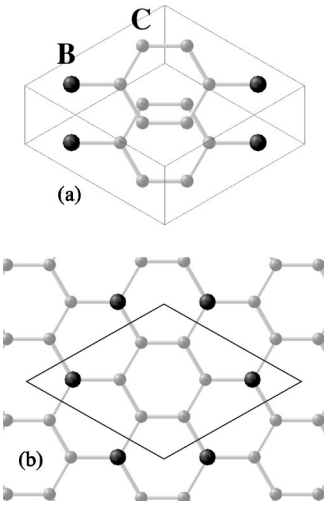

FIG. 1. Top views of the BC_3 structure with *ABC* stacking. In (a) two superimposed unit cells are viewed directly from above and in (b) a single layer of atoms is shown. The calculated in-plane lattice constant is 5.13 Å and the interlayer distance is 3.13 Å. Each layer is shifted relatively to the one below by 1.86 Å in the *y* direction. The layer shift breaks the rotational symmetry of the crystal and the relaxed angle between the in-plane lattice vectors is 60.1°.

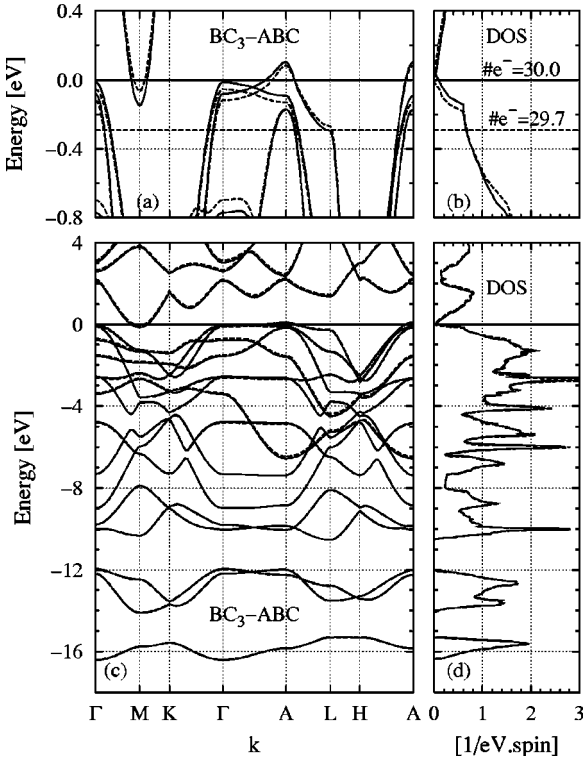

FIG. 2. Calculated electronic (a) and (c) bandstructure and (b) and (d) density of states of BC_3 for zero doping (solid lines) and 0.3 holes/unit cell (dashed lines). Figures (a) and (b) are blown-up versions of (c) and (d), respectively, in a narrow energy window around the Fermi level. The horizontal solid (dashed) line is at the zero doping (0.3 holes/cell) Fermi level.

electronic levels are filled. A background negative charge is applied to achieve charge neutrality. This method is compared to a rigid-band model. For the doped calculation the stresses and forces are very small, and no relaxation of the lattice parameters is carried out. Experimentally, the doping could be achieved either by chemically doping the system with charge acceptors or by gating the sample.

In Fig. 2 the LDA electronic band structure and density of states (DOS) of *ABC*-stacking BC_3 are shown for two doping levels: the zero doping case (solid lines) and the highest doping studied, 0.3 holes/unit cell (dashed lines). In Figs. 2(a) and 2(b) it is clear that the hole doping causes some of the bands, but not all, to shift by as much as 50 meV. Also, it is clear that the DOS at the Fermi level increases sharply with hole doping, which has a dramatic effect on superconductivity.

The phonon density of states $F(\omega)$ and the isotropic Eliashberg function $\alpha^2F(\omega)$ are shown in Figs. 3(a) and 3(b) for the case of 0.3 holes/cell. These are given by

$$F(\omega) = \sum_j \delta(\omega - \omega_{\mathbf{q}}^j), \tag{1}$$

$$\alpha^2F_j(\omega) = N(E_F) \sum_{\mathbf{k},\mathbf{k}'} W_{\mathbf{k}} W_{\mathbf{k}'} |\langle \mathbf{k}| \delta V_{\mathbf{q}}^j |\mathbf{k}'\rangle|^2 \delta(\omega - \omega_{\mathbf{q}}^j), \tag{2}$$

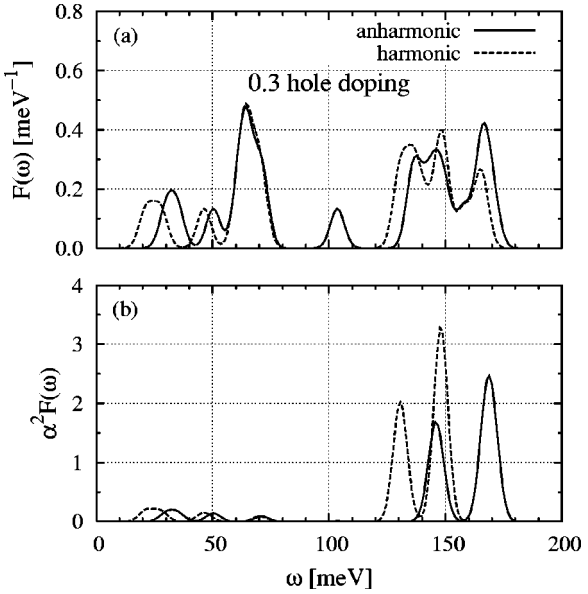

FIG. 3. (a) Phonon density of states $F(\omega)$ and (b) the isotropic Eliashberg function $\alpha^2F(\omega)$ calculated for anharmonic (solid lines) and harmonic (dashed lines) phonons.

$$\alpha^2F(\omega) = \sum_j \alpha^2F_j(\omega), \tag{3}$$

where $\mathbf{k}$ and $\mathbf{k}'$ label electronic states, $\omega_{\mathbf{q}}^j$ is the frequency of the phonon mode j and wave vector $\mathbf{q}=\mathbf{k}-\mathbf{k}'$, $N(E_F)$ is the electron density of states per spin at the Fermi level $W_{\mathbf{k}} = \delta(E_F - E_{\mathbf{k}})/N(E_F)$ and $\delta V_{\mathbf{q}}^j$ is the change in the crystal potential with and without a frozen phonon. Because only the $\mathbf{q}=\Gamma$ phonons were calculated, both $F(\omega)$ and $\alpha^2F(\omega)$ are discrete collections of $\delta(\omega-\omega_j)$ functions. For clarity, in the plots we have convoluted these functions with a gaussian having a 3 meV standard deviation. Figure 3(a) shows the role of anharmonicity. Most of the phonon modes are harmonic, but for some the anharmonicity is strong enough to raise the phonon frequencies by as much as 20 meV. The isotropic Eliashberg function contains an averaging of the EP couplings over all phonon frequencies. Figure 3(b) reveals that a few high frequency modes couple strongly with the electrons. Further inspection reveals that one of these strong coupling anharmonic modes is equivalent to the doubly degenerate bond stretching E_{2g} mode in MgB_2 that is very strongly coupled to the σ-bonding electrons.

The EP coupling constant λ is given by

$$\lambda = \int_0^\infty \alpha^2F(\omega)\frac{2}{\omega}d\omega, \tag{4}$$

$$= \sum_j \int_0^\infty \alpha^2F_j(\omega)\frac{2}{\omega}d\omega, \tag{5}$$

$$= \sum_j \lambda_j. \tag{6}$$

Table I shows values for selected modes for the 0.3 holes/cell doping case. Although the *ABC*-stacking of

TABLE I. The electron-phonon coupling constant for some phonon modes for both the harmonic and anharmonic cases assuming 0.3 holes/cell doping. The symmetry notations refer to the D_{6h} symmetry of an isolated sheet. The bracketed labels distinguish between different phonon polarizations with the same symmetry group.

	Harmonic		Anharmonic	
Mode	ω [meV]	λ_j	ω [meV]	λ_j
$E_{1g}[1]$	21.5	0.133	30.1	0.068
$E_{1g}[2]$	27.6	0.095	34.8	0.059
$B_{1g}[a]$	46.3	0.049	50.3	0.042
$E_{2g}[b1]$	131.1	0.119	144.7	0.097
$E_{2g}[b2]$	130.1	0.117	147.2	0.091
$E_{2g}[c1]$	147.9	0.185	167.3	0.144
$E_{2g}[c2]$	148.2	0.147	170.6	0.111

the BC_3 layers breaks the D_{6h} symmetry, the phonon polarizations remain very close to those for an isolated layer, especially for the in-plane modes. For this reason, the symmetry notations are retained here. However, the degeneracies of some modes are lifted as can be seen in Table I. What is also noticeable in Table I is that there are essentially six or seven modes that give a significant contribution to λ. The high frequency modes E_{2g-b1}, E_{2g-b2}, E_{2g-c1}, and E_{2g-c2} are in plane modes, while the low-frequency, E_{1g-2}, E_{1g-1}, and B_{1g-a} are out of plane modes. The latter are responsible for the low-frequency tail in $\alpha^2F(\omega)$ in Fig. 3. Because of the factor $1/\omega$ in equation 4, these modes have a strong contribution to the coupling constant λ. Compared to the frequency of 76 meV of the E_{2g} mode of MgB_2,[6] the bond stretching modes of BC_3 have much higher frequencies (147–170 meV), which, because of the $1/\omega$ factor, reduce their contribution to λ.

The phonon frequencies for all modes have been calculated for different doping levels. Figure 4(a) shows the dependence on doping of selected strong-coupling modes. It is interesting to notice that while for some modes the harmonic frequencies change significantly with doping, the anharmonic frequencies show much less variation.

The EP coupling λ was calculated in two ways. One approach did not involve doping, just a rigid-band shift. The dependence on the number of holes is caused by the variation of the Fermi level and the resulting changes in $N(E_F)$, and $W_{\mathbf{k}}$. The other approach was to calculate the EP matrices for each doping level. In Fig. 4(b) the effect on λ for both calculations is shown. Because in the undoped, rigid-band case the anharmonicity of the strong coupling modes is small, the undoped calculation of λ (dashed lines) for the harmonic and anharmonic cases gives essentially the same result. The doped calculation (solid lines), on the other hand, shows that the doping does have an effect probably due to the lowering of the phonon frequencies. In fact, if anharmonicity is neglected, λ would be increasingly overestimated with doping.

Finally, in Fig. 5 the dependence of the superconducting temperature on doping and anharmonicity is shown. The superconducting transition temperature T_c has been calculated with the McMillan equation[18–20]

$$T_c = \frac{\omega_{\ln}}{1.2}\exp\frac{-1.04(1+\lambda)}{\lambda-\mu^*(1+0.62\lambda)}, \tag{7}$$

where $\omega_{\ln}$ is the logarithmic average of the phonon frequency and μ^* is the Coulomb pseudopotential parameter. Typical values of μ^* were used: 0.10, 0.12, and 0.14. Our results suggest that the maximum T_c should lie between 16 and 30 K at a doping level of 0.2 to 0.3 holes/cell. Figure 5(a) shows the anharmonic results and Fig. 5(b) displays the harmonic case. As was found for λ, failure to include anhar-

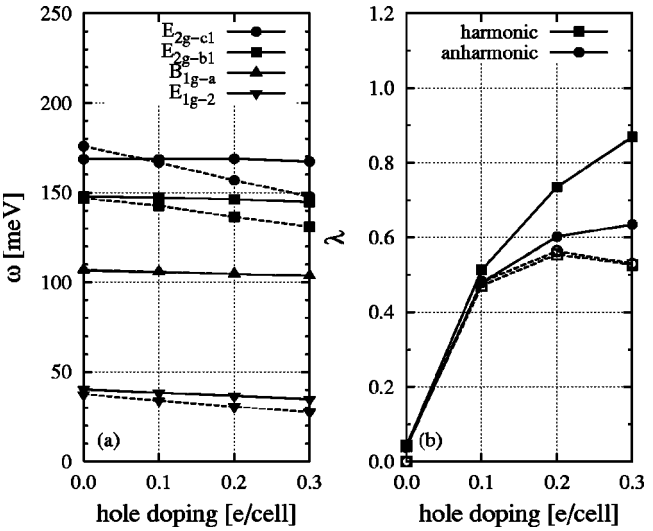

FIG. 4. (a) Selected phonon frequencies as a function of doping. Solid (dashed) lines for anharmonic (harmonic) frequencies. (b) calculated EP coupling constant λ as a function of doping. The solid lines represent the fully doped calculation, while the dashed lines are for the non-doped calculation (see text).

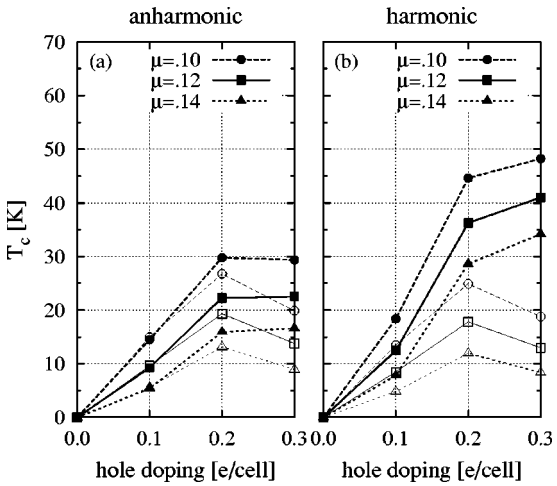

FIG. 5. The superconducting temperature T_c as a function of doping level calculated using (a) the anharmonic and (b) harmonic phonon frequencies, and for different values of μ^*. Full (empty) markers indicate that the electron-phonon matrix elements were calculated with doping (no doping). See text for details.

monic effects in the doped calculation leads to an overestimation of T_c. The undoped results are similar to the doped case, although a sharp decrease in T_c at 0.3 holes/cell is observed. This is connected to the decrease in λ at the same doping level.

In conclusion, we have shown that for the metallic *ABC*-stacking BC_3 structure, superconductivity at a T_c of about 22 K can be achieved with doping levels of 0.2 to 0.3 holes/cell. The high frequency phonon modes that couple strongly to the electrons are in-plane, bond-stretching modes, very similar to the E_{2g} mode in MgB_2. In addition, three out-of-plane modes contribute significantly to T_c, mainly due to their very low frequency. The effect of anharmonicity has been taken into account. This leads to an attenuation of the EP coupling constant λ, and consequently, of T_c. However, if anharmonicity is not uniform throughout the Brillouin zone, the attenuation of the EP coupling could be weaker, leading to an underestimation of T_c. On the other hand, since only zone-center phonons were calculated, if the EP coupling is peaked at Γ, T_c could be overestimated. The dependence of the phonon spectrum on doping was calculated and it was shown that the corrections to the frequencies are relatively small.

We would also like to point out that the specific stacking of the BC_3 layers should not significantly affect superconductivity. The band structures of all the stackings studied previously[11] show that the top of the σ bands are located very close to the Fermi level. Hole doping BC_3 in any of the possible stackings lowers the Fermi level below the top of the σ bands. This leads to the strong electron-phonon coupling between the σ-band electrons at the Fermi surface with the in-plane phonon modes, which is the main contribution to λ and T_c. Therefore, superconductivity is expected in hole doped BC_3 regardless of the layer stacking.

We would like to thank Dr. Hyoung Joon Choi for his valuable comments and interesting discussions. This work was supported by the National Science Foundation under Grant No. DMR-0087088, and by the Office of Energy Research, Office of Basic Energy Sciences, Materials Sciences Division of the U.S. Department of Energy under Contract No. DE-AC03-76SF00098. Computational Resources were provided by NPACI and by NERSC.

[1] J. Nagamatsu, N. Nakagawa, T. Muranaka, Y. Zenitani, and J. Akimitsu, Nature (London) **410**, 63 (2001).
[2] J. Kortus, I. Mazin, K. Belashchenko, V. Antropov, and L. Boyer, Phys. Rev. Lett. **86**, 4656 (2001).
[3] J. An and W. Pickett, Phys. Rev. Lett. **86**, 4366 (2001).
[4] K.-P. Bohnen, R. Heid, and B. Renker, Phys. Rev. Lett. **86**, 5771 (2001).
[5] H. J. Choi, D. Roundy, H. Sun, M. L. Cohen, and S. G. Louie, Nature (London) **418**, 758 (2002).
[6] H. J. Choi, D. Roundy, H. Sun, M. L. Cohen, and S. G. Louie, Phys. Rev. B **66**, 020513(R) (2002).
[7] J. Kouvetakis, R. Kaner, M. L. Sattler, and N. Bartlett, J. Chem. Soc., Chem. Commun. **1986**, 1758.
[8] R. M. Wentzcovitch, M. L. Cohen, S. G. Louie, and D. Tománek, Solid State Commun. **67**, 515 (1988).
[9] D. Tománek, R. M. Wentzcovitch, M. L. Cohen, and S. G. Louie, Phys. Rev. B **37**, 3134 (1988).
[10] K. M. Krishnan, Appl. Phys. Lett. **58**, 1857 (1991).
[11] H. Sun, F. J. Ribeiro, J.-L. Li, D. Roundy, M. L. Cohen, and S. G. Louie, Phys. Rev. B **69**, 024110 (2004).
[12] M. L. Cohen, Phys. Scr. **T1**, 5 (1982).
[13] D. M. Ceperley and B. J. Alder, Phys. Rev. Lett. **45**, 566 (1980).
[14] L. Kleinman and D. M. Bylander, Phys. Rev. Lett. **48**, 1425 (1982).
[15] J. L. Martins, N. Troullier, and S.-H. Wei, Phys. Rev. B **43**, 2213 (1991).
[16] P. K. Lam and M. L. Cohen, Phys. Rev. B **25**, 6139 (1982).
[17] M. M. Dacorogna, M. L. Cohen, and P. K. Lam, Phys. Rev. Lett. **55**, 837 (1985).
[18] W. McMillan, Phys. Rev. **167**, 331 (1968).
[19] P. Allen and R. Dynes, Phys. Rev. B **12**, 905 (1975).
[20] J. Carbotte, Rev. Mod. Phys. **62**, 1027 (1990).